EPJ Web of Conferences **95**, 03018 (2015)
DOI: 10.1051/epjconf/20159503018

Hot and cold nuclear matter effects in p–Pb collisions at the LHC

Jason Kamin[1,a]

[1] *Frankfurt Institute for Advanced Studies, Goethe-Universität Frankfurt am Main, Germany*

Abstract. The pA system is typically regarded in heavy ion collisions as a "cold" nuclear matter environment and thought to isolate and identify initial state effects due to the presence of multiple nucleons in the incoming nucleus. Moreover, pA collisions bridge the gap between peripheral AA collisions and the pp baseline to create a more complete understanding of underlying production mechanisms and how they evolve with multiplicity. Recent measurements at both RHIC and the LHC provide an indication, however, that the "cold" nuclear matter picture may be somewhat naïve.
Recent LHC results from the 2013 p–Pb run at $\sqrt{s_{NN}}$ = 5.02 TeV will be discussed.

1 Introduction

In order to study the quark-gluon plasma (QGP) created in heavy-ion collisions at both RHIC and the LHC, it is useful to analyze pp collisions to establish a comparable baseline for observables. Moreover, to isolate any initial state that may be present, pA (or dA at RHIC) collisions are studied. The pA energy density is believed to be too low to create a thermalized medium thereby making it an ideal control environment. The presence of additional nuclear matter (relative to pp collisions) can alter the incoming wavefunction of the nucleus leading to modified observables. These collectively referred to as "cold nuclear matter" effects.

It was therefore a surprise was pA collisions began to reveal unexpected phenomena with respect to pp collisions [1–3]. In the highest multiplicity events (collisions with the smallest impact parameter) collective effects were observed, implying that there might be a thermalized medium being formed in these smaller systems. Moreover, a high p_{T} *enhancement* with respect to pp collisions is seen contrasting the typical *suppression* in AA collisions. pA collisions also provide a testing ground for pQCD in heavy flavor measurements illuminating nuclear shadowing (and antishadowing) for these hard probes. Finally, at higher Q^2 the electroweak bosons directly reflect pQCD processes and can give an indication of initial state nuclear modification as well as even potentially providing a centrality calibration.

The LHC is capable of providing simultaneous p and Pb beams with an asymmetric center-of-momentum collision frame. After a short, four hour pilot p–Pb run (1 $\mu\mathrm{b}^{-1}$) in September 2012, the LHC delivered 35 $n\mathrm{b}^{-1}$ over a 3 week span in January 2013. A 4 TeV proton beam colliding with a 1.57 TeV/nucleon Pb beam results in $\sqrt{s_{NN}}$ = 5.02 TeV collisions that are shifted by $\Delta y = 0.465$ in the direction of the proton.

[a] e-mail: jason.kamin@cern.ch

2 Collective Effects

Thermodynamic systems are characterized by comprising a large number of particles (typically $> 10^4$) in local thermal equilibrium. This distinction between a system of individual particles and a medium in which individual degrees of freedom do not matter anymore is relevant when comparing pp collisions ($\mathrm{d}N_{ch}/\mathrm{d}\eta \approx 6$) and central Pb–Pb collisions ($\mathrm{d}N_{ch}/\mathrm{d}\eta \approx 1600$). According to fast simulations, to reach thermal equilibrium between the constituents, the lifetime of the system should be on the order of 3 – 6 interactions.

The success of hydrodynamic models to describe the flow-like phenomena observed in Pb–Pb collisions supports the idea that the QGP is in local *kinetic* equilibrium. Meanwhile, their success in also describing hadron yields indicates that the hot matter is in local *chemical* equilibrium. To understand the onset of these collective effects, searches are ongoing for these phenomena in pA systems as well.

2.1 Radial Flow

[4]

Isotropic radial flow is a uniform medium expansion that drives all particles towards a constant expansion velocity. This naturally results in a mass hierarchy for the p_{T} distributions; lower mass particles are pushed to higher transverse momentum. The p_{T} distributions for various particle species produced in p–Pb collisions at $\sqrt{s_{\mathrm{NN}}} = 5.02$ TeV are shown in Fig. 1 and compared to DPMJet[1], a QCD-based simulation as well as two hydrodynamic models (EPOS[2] and Krakow[3]). Both show better agreement than the DPMJet. In addition, a Blast-Wave [5] (a simplified hydrodynamics model) fit simultaneously to all data points can qualitatively describe the data as well.

The Blast-Wave fit contains two interpretable parameters, T_{kin} (the common kinetic freeze-out temperature) and $< \beta_T >$ (the collective average expansion velocity). Figure 2 plots these against each other for various systems. The centrality (or charged particle multiplicity) increases from left to right. The correlation seen in Pb–Pb (red points) is characteristic of collective behavior resulting from a thermalized expanding medium. The T_{kin} is related to the lifetime of the system; a longer-lived medium has a lower time-averaged temperature since the system is cooling as it expands. Therefore, more peripheral collisions, being shorter-lived, wind up with a *higher* T_{kin} as well as a *smaller* expansion velocity. More central Pb–Pb collisions have a *lower* T_{kin} and *larger* expansion velocity. Notably, both p–Pb (dark blue circles) and pp (black triangles) systems exhibit similar behavior indicating collective expansion in these small systems. PYTHIA (open light blue squares) does not reveal any correlation between these parameters. However, PYTHIA with c̈olor reconnectionb̈egins to qualitatively approximate the correlated trend, hinting that it could be possible to mimick flow-like patterns without invoking hydrodynamics.

2.2 Elliptic Flow

Two particle "jet like" correlations are expected and observed in all systems (pp , pA , and AA) via a double peak structure in $\Delta\phi$. Fig. 3 shows this two-dimensional distribution for p–Pb collisions. The near-side peak ($\Delta\phi \approx 0$) is reasonably peaked in $\Delta\eta$, fully representing a jet. The away-side jet is peaked around $\Delta\phi \approx \pi$ but smeared out in $\Delta\eta$. The left panel is for more peripheral events while the right is for more central (estimated by the number of charged tracks).

[1] https://wiki.bnl.gov/eic/index.php/DPMJet

[2] K.Werner et al. ArXiv:1004.0805

[3] P. Bozek, M. Chojnacki, W. Florkowski, B. Tomasik, Phys. Lett. B694 (2010) 238–241

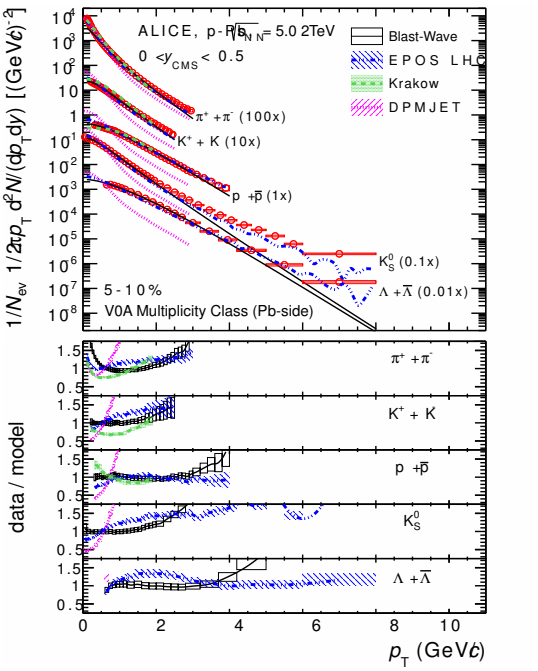

Figure 1. Pion, kaon, and proton transverse momentum distributions in the 5-10% V0A multiplicity class measured in the rapidity interval $0 < y_{\mathrm{CMS}} < 0.5$ compared to the several models.

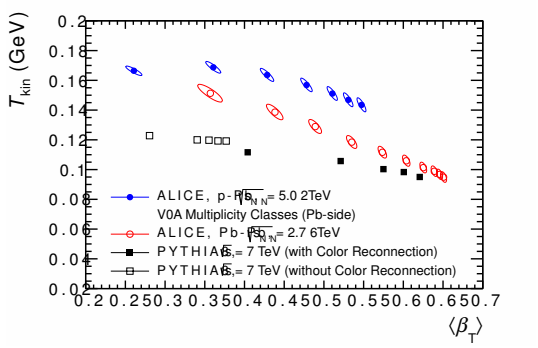

Figure 2. Results of blast-wave fits, compared to Pb–Pb data and MC simulations from PYTHIA8 with and without color reconnection. Charged-particle multiplicity increases from left to right. Uncertainties from the global fit are shown as correlation ellipses.

The interesting feature is in the higher multiplicity events; a near-side ridge extending along $\Delta\eta$, which is typically interpreted as an elliptic flow effect in AA collisions, can be seen in Fig. 3 [6]. Moreover, to isolate this feature, in Fig. 4 the most peripheral events are subtracted from the most central. The resulting distribution clearly shows a double ridge structure indicating long range, non

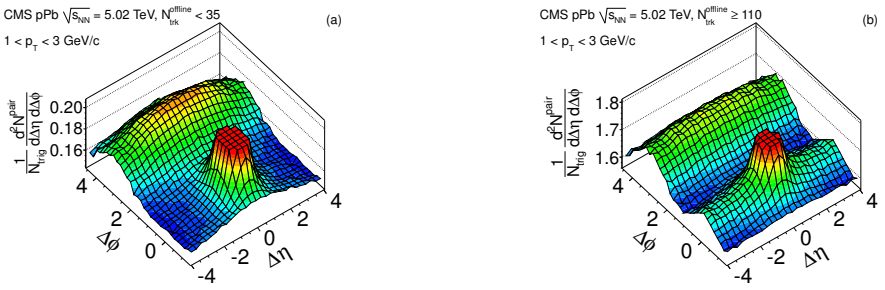

Figure 3. Associated yield for the near-side of the correlation function averaged over $2 < |\Delta\eta| < 4$ and integrated over the region $|\Delta\phi| < 1.2$ in 7 TeV pp collisions (open circles) and 5.02 TeV p–Pb collisions (solid circles). Panel (a) shows the associated yield as a function of p_{T} for events with $N_{\mathrm{trk}}^{\mathrm{offline}} \geq 110$. In panel (b) the associated yield for $1 < p_{\mathrm{T}} < 2\mathrm{GeV}/c$ is shown as a function of multiplicity $N_{\mathrm{trk}}^{\mathrm{offline}}$. The p_{T} selection applies to both particles in each pair. The error bars correspond to statistical uncertainties, while the shaded areas denote the systematic uncertainties.

jet-like correlations in p–Pb . A Fourier decomposition of the projected $\Delta\phi$ distribution (right panel) shows that it's dominated by the second and third Fourier coefficients, v_2 and v_3.

$$v_n = \langle \cos n(\phi - \Psi_n) \rangle \tag{1}$$

These Fourier coefficients are believed to be driven by the original collision geometry (and hence the medium's initial shape). Traditionally in heavy ion collisions, an almond-like shape made by two overlapping circles is imagined to create an azimuthally asymmetric pressure gradient. This gradient then causes the medium to expand more forcefully along the shorter geometric axis (where the gradient is largest) creating an azimuthally asymmetric p_{T} distribution. This asymmetry is considered to be medium-induced elliptic flow and is not understood in p–Pb collisions, which are believed to not have any initial medium geometry. [7]

In addition, a mass ordering of the v_2 is observed and shown in Fig. 5. The left panel is central p–Pb data that hints at a mass-ordered trend of v_2 [21]. This trend is further illustrated in the right panel by subtracting the peripheral collisions from the central collisions [22]. This mass ordering trend is also seen in Pb–Pb collisions [8] and is considered a hydrodynamic signature; elliptic flow of particles is driven by the expansion velocity of the medium, translating to the momentum of the various particles proportional to their mass ($p_{\mathrm{T}} = \beta_{\mathrm{T}}\gamma m$).

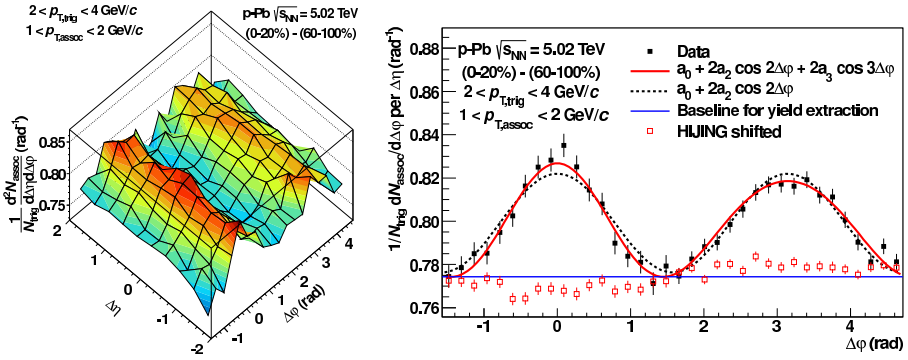

Figure 4. Left: Associated yield per trigger particle in $\Delta\phi$ and $\Delta\eta$ for pairs of charged particles with $2 < p_{\mathrm{T,trig}} < 4$ GeV/c and $1 < p_{\mathrm{T,assoc}} < 2$ GeV/c in p–Pb collisions at $\sqrt{s_{\mathrm{NN}}} = 5.02$ TeV for the 0–20% multiplicity class, after subtraction of the associated yield obtained in the 60–100% event class. Right: Same distribution projected onto $\Delta\phi$ averaged over $0.8 < |\Delta\eta| < 1.8$ on the near side and $|\Delta\eta| < 1.8$ on the away side. Superimposed are fits containing a $\cos(2\Delta\phi)$ shape alone (black dashed line) and a combination of $\cos(2\Delta\phi)$ and $\cos(3\Delta\phi)$ shapes (red solid line). The blue horizontal line shows the baseline obtained from the latter fit which is used for the yield calculation. Also shown for comparison is the subtracted associated yield when the same procedure is applied on HIJING shifted to the same baseline. The figure shows only statistical uncertainties. Systematic uncertainties are mostly correlated and affect the baseline. Uncorrelated uncertainties are less than 1%. [7]

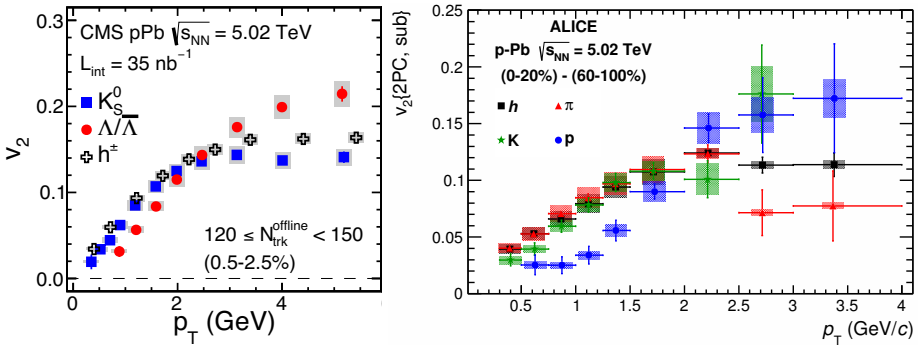

Figure 5. Left: CMS v_2 results for K^0_s (filled squares), $\Lambda/\bar{\Lambda}$ (filled circles), and inclusive charged particles (open crosses) as a function of p_{T} for four multiplicity ranges obtained from high-multiplicity triggered p–Pb sample at $\sqrt{s_{\mathrm{NN}}} = 5.02$ TeV. [21] Right: ALICE Fourier coefficient v2{2PC,sub} for hadrons (black squares), pions (red triangles), kaons (green stars) and protons (blue circles) from the correlation in the 0–20% multiplicity class after subtraction of the correlation from the 60–100% multiplicity class. [22]

3 High p_{T} Enhancement

The Nuclear Modification Factor, R_{AA}, quantifies the spectral modification of a distribution due to nuclear effects in AA collisions. Likewise R_{pA} is the pA equivalent:

$$R_{pA} = \frac{dN_{pA}/dp_T}{\langle N_{coll}\rangle dN_{pp}/dp_T} \tag{2}$$

R_{pA} gives information about how different pA collisions are with respect to a superposition of many pp collisions. An R_{pA} of unity indicates no modification from the appropriate number of binary pp collisions (N_{coll}) and no cold nuclear effects. R_{pA} typically exhibits an enhancement of high momentum particles referred to as the Cronin Effect [9]. The effect is generally considered to be a result of multiple soft scattering of the incoming partons as they propagate thorugh the target nucleus [10]. The average number of binary collisions is calculated using a Glauber model and in p–Pb is $\langle N_{coll}\rangle = 6.9 \pm 0.6$ [11].

The Cronin Effect is observed to be strongly mass dependent. R_{pPb} for various particle species are is shown in Fig. 6. This hardening of the p_{T} distribution is qualitatively consistent with the radial flow picture, further supporting the idea that the p–Pb system exhibits some collective behavior. In addition, RHIC data are qualitatively consistent with this observation and interpretation [12].

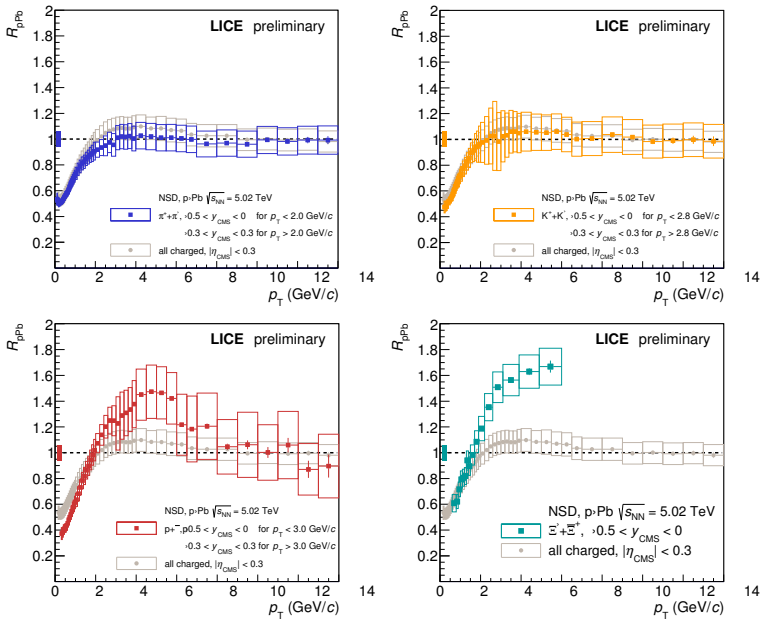

Figure 6. Nuclear Modification Factor in p–Pb collisions for charged π, K, p, and Ξ.

As the single identified particle R_{pPb} data tend to flatten and trend towards unity at high p_{T} (> 10 GeV/c), the expectation from pQCD is for this trend to continue and not deviate from unity at even higher p_{T} . However, when looking at unidentified charged particles (right panel of Fig. 7), an unexplained rise in R_{pPb} is observed. This charged particle enhancement is measured by both the ATLAS and CMS collaborations. However, the ALICE collaboration hints at a different trend, closer to unity. It should be stressed that the ALICE data is statistics limited above 20 GeV/c and a conclusion about the trend of the data should be taken as such. Moreover, all three experiments have large systematic uncertainties making it difficult to arrive at a firm conclusion. In addition,

some modification is expected due to anti-shadowing [13], though not nearly enough to explain the enhancement seen by ATLAS and CMS.

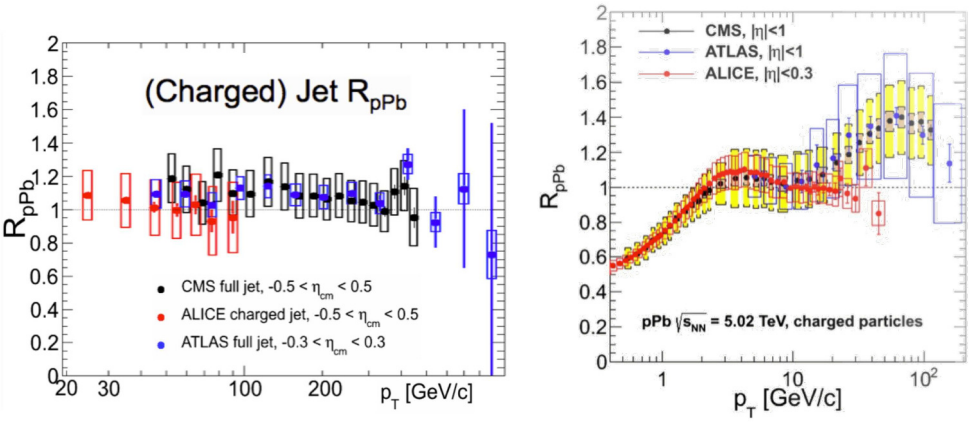

Figure 7. Left: $R_{pPb}$of charged jets from CMS, ATLAS, and ALICE. Right: Overlaid CMS, ATLAS, and ALICE measurements of $R_{pPb}$of unidentified c harged particles.

The apparent discrepancy between ATLAS/CMS and ALICE can be broken down further. Fig. 8 shows a comparison of the decomposition of the R_{pPb}between CMS and ALICE. The ratio of the p–Pb spectra is shown on the left while the ratio of the pp reference spectra is on the right. The ratios drift in opposite directions and moreover reveal that the bulk of the difference ($\sim {}^{2}/_{3}$) comes from the pp reference. As pp data do not exist at $\sqrt{s} = 5.02$ TeV, an interpolation is used from $\sqrt{s} = 2.76$ TeV and $\sqrt{s} = 7$ TeV, carrying with it a large systematic uncertainty. A pp reference run at $\sqrt{s} = 5.02$ TeV during Run 2 of the LHC would significantly help in reducing this uncertainty on the reference for all experiments.

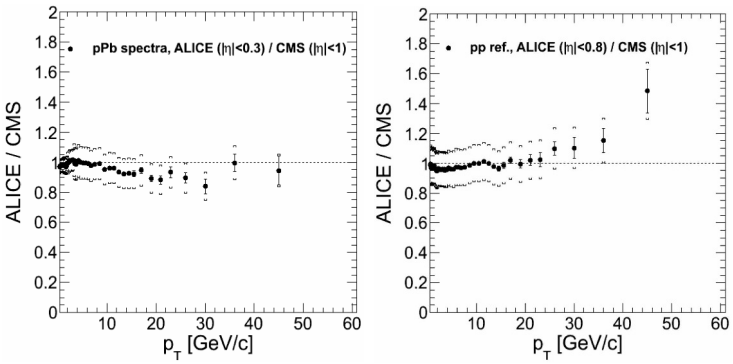

Figure 8. Comparing the unidentified charged particle p_T spectra from ALICE and CMS for p–Pb (left) and pp (right).

Another point worth noting is that the $R_{pPb}$for charged jets in CMS, ALICE, and ATLAS are in full agreement and fully consistent with unity (shown in the left panel of Fig. 7). This might imply that any rise in the unidentified charged particles could be due to the fragmentation functions, which translate how the jets fragment into the vacuum. However, fragmentation functions are generally considered to be quite under control.

4 Heavy Flavor

Precise measurements of quarkonia are crucial to understand hot and cold nuclear matter and to probe de-confinement in QGP matter. There are two major and competing efects in AA collisions. *Thermal dissociation* refers to bound states being broken up by the QGP. *Statistical regeneration* happens when one quark in the medium randomly "finds" another nearby to form a resonance. The interpretation in AA collisions is reliant on disentangling any pA effects such as PDF modifications inside the nuclei (shadowing), gluon saturation, energy loss, or nuclear absorption. In addition, heavy flavor studies can help to constrain the incoming nuclear PDFs.

4.1 J/ψ

The top panel in Fig. 9 shows the $R_{pPb}$for inclusive J/ψ as a function of center-of-mass rapidity [14]. There is an observed suppression at positive y (p-going direction), which probes the low-x partons in the Pb nucleus. Conversely, there is little modification in the Pb-going direction. The lower panels (left-to-right) show the p_{T} dependence of the negative and positive rapidities respectively showing that the suppression is mainly at low p_{T} . The data are in reasonable agreement with current models; NLO with EPS09 shadowing and coherent energy loss seem to work the best with CGC models more questionable. Fig. 10 shows LHCb measurements in agreement as well [15].

The theoretical uncertainties for the EPS09 NLO calculation [16] are due to the uncertainty on the EPS09 shadowing parameterization and to the mass and scale uncertainties on the cross section calculation. For the CGC model [18], the band is related to the choice of the parton saturation scale and of the charm quark mass. Finally, the q_0 value in the energy loss model [17] represents the value of the transport coefficient in the target nucleons for x_{Bj}=10^{-2} gluons.

4.2 Relative $\psi\prime$ Suppression

The naive expectation for the $\psi\prime$ is for the suppression to match that of the J/ψ. However, Fig. 11 shows the $R_{pPb}$for both states, revealing that the $\psi\prime$ is, in fact, *more* suppressed than the J/ψ, particularly in the Pb-going direction [19]. In addition, Fig. 12 show that the double ratio of $R_{pA}(\psi(2S))/R_{pA}(\psi(1S))$ is compatible with $\sqrt{s_{NN}}$ = 200 GeV measurements at RHIC [20]. Since models predict similar behavior for both states, this could hint at a final state effect– even in pA . This result is particularly unexpected since the charmonia formation time is *larger* than the $c\bar{c}$ crossing time in a nucleus.

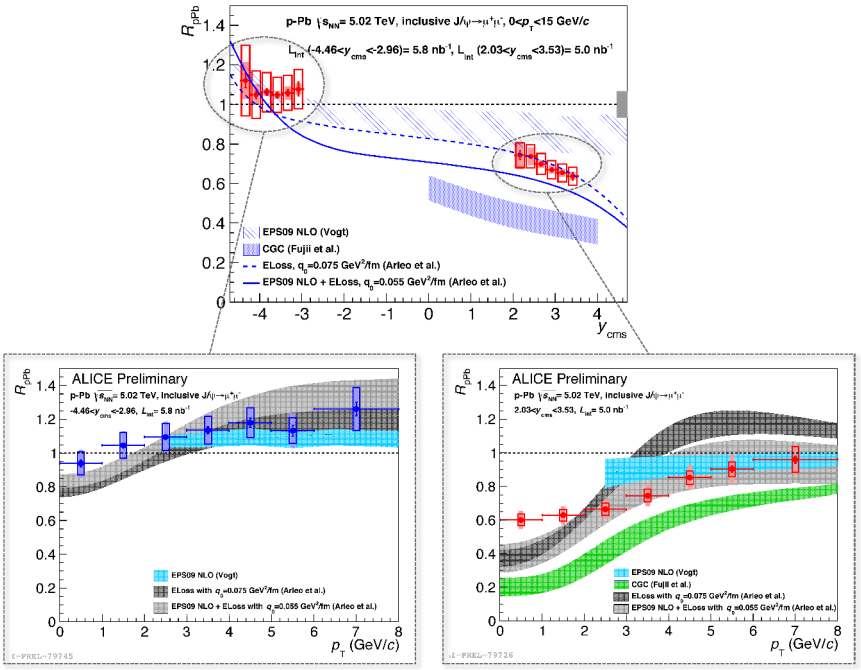

Figure 9. The nuclear modification factors for inclusive J/ψ production at $\sqrt{s_{\rm NN}}$ = 5.02 TeV [14]. Results from various models are also shown.

5 Electroweak Bosons

Electroweak bosons are convenient measurements in p–Pb collisions as they are sensitive to nuclear PDF modifications but not fianl state effects. This makes them a clean probe to understand p–Pb scaling properties and establish a nuclear baseline.

5.1 Z^0

ATLAS, CMS, and LHCb have measured Z^0 production in p–Pb collisions; ATLAS observes $\sim$ 3500, CMS sees $\sim$ 1600, and LHCb observes $\sim$ 15. The left panel of Fig. 13 shows shows the differential cross section in ATLAS. Some modification compared to a simple pp(pn) scaling is observed at negative y. The right panel shows the forward/backward asymmetry from CMS in agreement with models and can be used to constrain nuclear PDFs.

Z^0 production is not expected to be modified by any medium effects. Therefore, when looking differentially in centrality, it is expected to directly scale with the number of binary collisions. Fig. 14 compares two different centrality approaches.

5.2 $W^{\pm}$

ALICE has measured W production via the cross section of muons and find it to be consistent with binary scaling expectations (left panel of Fig. 15). The right panel of Fig. 15 attempts to compare different centrality estimations, finding them all consistent within the uncertainties.

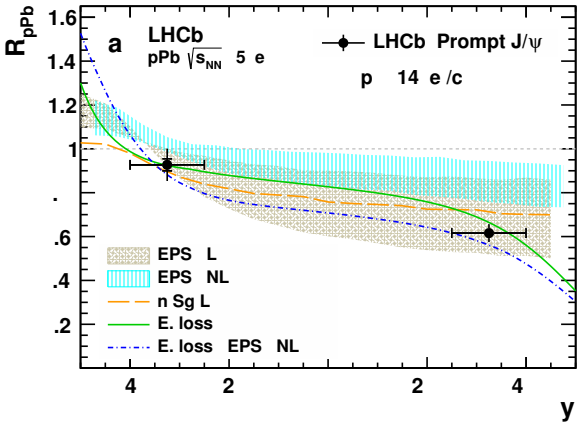

Figure 10. The nuclear modification factors for inclusive J/ψ production at $\sqrt{s_{\rm NN}}$ = 5.02 TeV at LHCb [15].

Fig. 16 shows the charge asymmetry (left panel) and forward/backward asymmetry (right panel) of W production measured at CMS. They reveal some deviations from unmodified PDFs, while EPS09-modified nuclear PDFs are closer to the data. This could hint at needing different modifications for u and d quarks that don't exist in EPS09, though the evidence is not convincing.

6 Summary

p–Pb collisions explore many interesting, unexpected physics questions and are establishing themselves as a legitimate probe of the nuclear environment, beyond a simple control experiment for AA collisions. Many medium-like features have been observed for most particles at low $p_{\rm T}$ including elliptic flow and radial flow as well as the success of thermal models to fit the data. While there is no indication of any suppression at high $p_{\rm T}$ (as in AA), there is an interesting enhancment of charged particles at high $p_{\rm T}$ that is still unexplained. In addition, quarkonia measurements continue to provide the essential baseline for Pb–Pb while eletroweak boson can help to constrain nuclear PDFs and centrality estimators. Certainly, the second run of the LHC beginning in 2015 will pick up where Run 1 left off and help reveal even more about these high multiplicity, small systems.

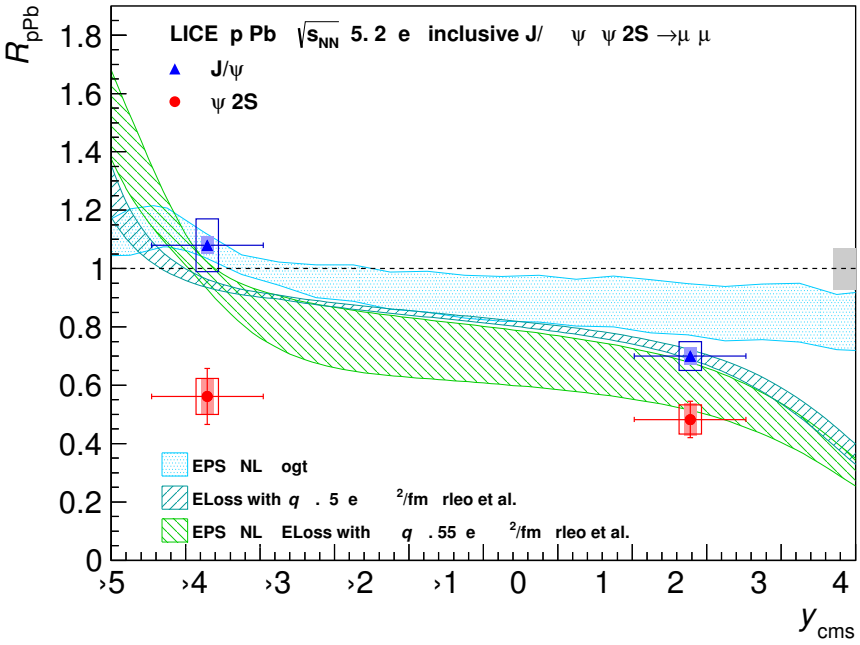

Figure 11. $R_{pPb}$for the J/ψ (blue) and $\psi\prime$ (red) [19].

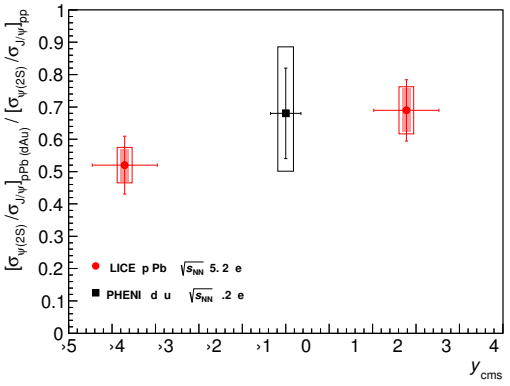

Figure 12. Double ratio of $R_{pA}(\psi(2S))/R_{pA}(\psi(1S))$ for LHC (red) and RHIC (black) energies [19].

References

[1] G. Aad, ALTAS Collaboration, *et al.*, Phys. Rev. Lett. **110**, 182302 (2013)
[2] B. Abelev, ALICE Collaboration, *et al.*, Phys. Lett. B **719**, 29 (2013)
[3] S. Chatrchyan, CMS Collaboration, *et al.*, Phys. Lett. B **724**, 213 (2013)
[4] B. Abelev, ALICE Collaboration, *et al.*, Phys. Lett. B **728**, 25-38 (2014)
[5] E. Schnedermann, J. Sollfrank, and U. W. Heinz, Phys. Rev. C **48**, 2462 (1993)

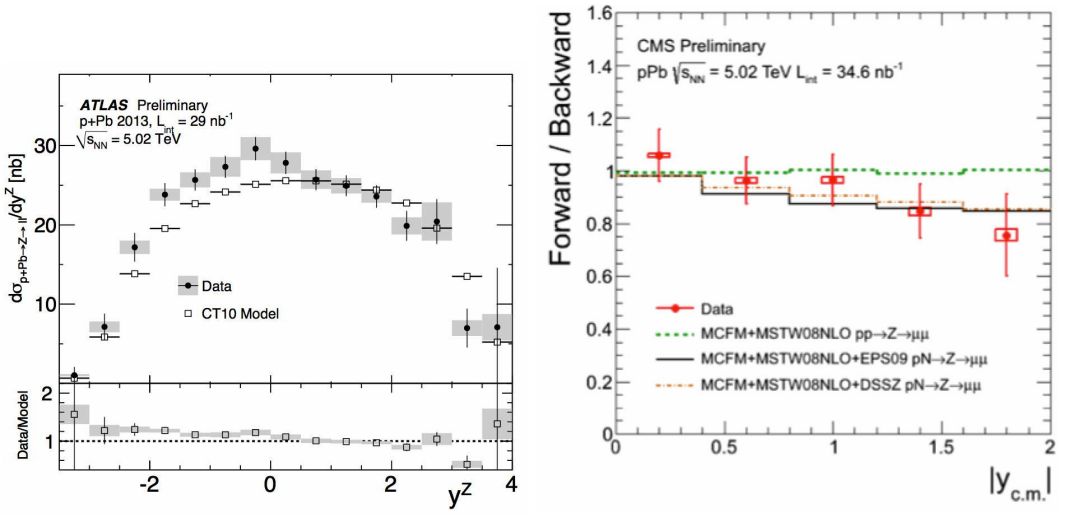

Figure 13. Left: Differential cross section for Z^0 production measured in ATLAS. Right: Forward/backward asymmetry measured in CMS.

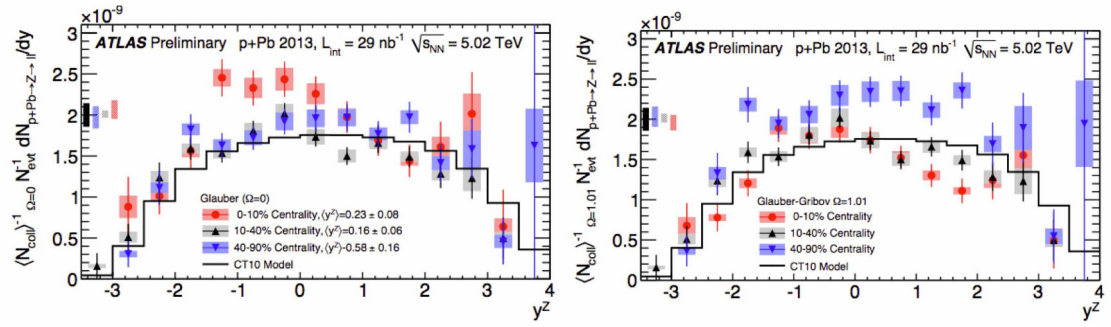

Figure 14. Comparing different centrality approaches using Z^0 production in p–Pb collisions.

[6] S. Chatrchyan, CMS Collaboration, *et al.*, Phys. Lett. B **718**, Issue 3, 795-814 (2013)

[7] B. Abelev, ALICE Collaboration, *et al.*, Phys. Lett. B **719**, 29 (2013)

[8] B. Abelev, ALICE Collaboration, *et al.*, Elliptic flow of identified hadrons in Pb-Pb collisions at $\sqrt{s_{NN}}$ = 2.76 TeV, *CERN-PH-EP-2014-104*

[9] J. W. Cronin *et al.*, Phys. Rev. D **11**, 3105 (1975).

[10] A. Accardi. Cronin efect in proton-nucleus collisions: A survey of theoretical models. *hep-ph/0212148*, (2000).

[11] J. Adam, ALICE Collaboration, *et al.* Centrality dependence of particle production in p–Pb collisions at $\sqrt{s_{NN}}$ = 5.02 TeV, *arXiv:1412.6828* (2014).

[12] S. Adler, PHENIX Collaboration, *et al.* Phys. Rev. C **74**, 024904 (2006).

[13] I. Helenius, *et al.* JHEP 1207 **073** (2012).

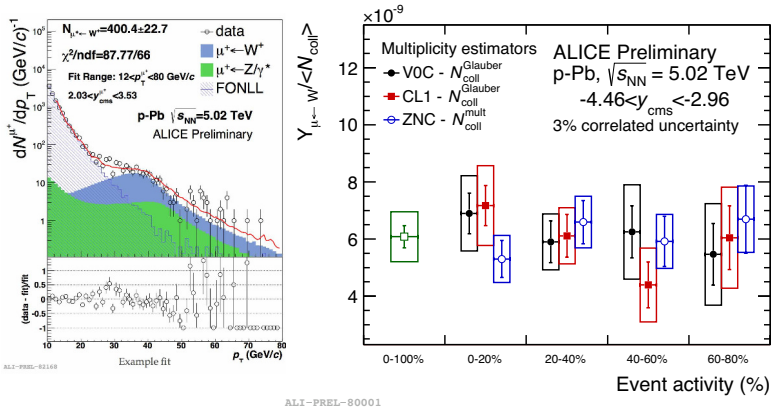

Figure 15. Left: Muon yield highlighting electroweak components at high p_T measured in ALICE. Right: Comparing different centrality estimators via W production in ALICE.

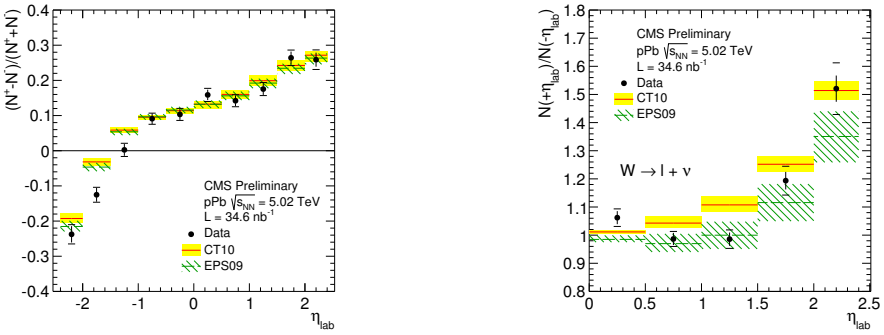

Figure 16. Left: Charge asymmetry of W production measured at CMS. Right: Forward/backward asymmetry measured in CMS.

[14] B. Abelev, ALICE Collaboration, *et al.*, JHEP 02 **073**, (2014)

[15] R. Aaij, LHCb Collaboration, *et al.*, JHEP 02 **072**, (2014)

[16] R. Vogt, Int. J. Mod. Phys. **E22**(2013) 1330007 and priv. comm.

[17] F. Arleo and S. Peigné, JHEP **1303**(2013) 122.

[18] H. Fujii and K. Watanabe, Nucl. Phys. **A915**(2013) 1.

[19] B. Abelev, ALICE Collaboration, *et al.*, Suppression of $\Psi\prime$(2S) production in p–Pb collisions at $\sqrt{s_{NN}}$ = 5.02 TeV (2014) *arXiv:1405.3796*

[20] A. Adare, PHENIX Collaboration, *et al.*, Phys. Rev. Lett. **111**, 202301 (2013)

[21] S. Chatrchyan, CMS Collaboration, *et al.*, submitted to Phys. Lett. B (2014), *arXiv:1409.3392*

[22] B. Abelev, ALICE Collaboration, *et al.*, Phys. Lett. B **726**, Issue 1-3, 164-177 (2013)

[23] S. Chatrchyan, CMS Collaboration, *et al.*, Study of W boson production in pPb collisions at $\sqrt{s_{NN}}$ = 5.02 TeV, *CMS-PAS-HIN-13-007*